Dissociation Potential Curves of Low-Lying States in Transition Metal Hydrides. 3. Hydrides of Groups 6 and 7

Shiro Koseki,*,† Takeshi Matsushita,†,‡ and Mark S. Gordon*,§

Department of Chemistry, Graduate School of Science, Osaka Prefecture University, 1-1 Gakuen-cho, Sakai, Osaka 599-8531, Japan, Chisso Corporation, 3-13-1 Kachidoki, Chuo-ku, Tokyo 104-8555, Japan, and Department of Chemistry and Ames Laboratory, Iowa State University, Ames, Iowa 50011

Received: October 31, 2005; In Final Form: December 22, 2005

The dissociation curves of low-lying spin-mixed states in monohydrides of groups 6 and 7 were calculated by using an effective core potential (ECP) approach. This approach is based on the multiconfiguration self-consistent field (MCSCF) method, followed by first-order configuration interaction (FOCI) calculations, in which the method employs an ECP basis set proposed by Stevens and co-workers (SBKJC) augmented by a set of polarization functions. Spin−orbit coupling (SOC) effects are estimated within the one-electron approximation by using effective nuclear charges, since SOC splittings obtained with the full Breit−Pauli Hamitonian are underestimated when ECP basis sets are used. The ground states of group 6 hydrides have $\Omega = {}^1/_2(X^6\Sigma^+_{1/2})$, where Ω is the z component of the total angular momentum quantum number. Although the ground states of group 7 hydrides have $\Omega = 0^+$, their main adiabatic components are different; the ground state in MnH originates from the lowest $^7\Sigma^+$, while in TcH and ReH the main component of the ground state is the lowest $^5\Sigma^+$. The present paper reports a comprehensive set of theoretical results including the dissociation energies, equilibrium distances, electronic transition energies, harmonic frequencies, anharmonicities, and rotational constants for several low-lying spin-mixed states in these hydrides. Transition dipole moments were also computed among the spin-mixed states and large peak positions of electronic transitions are suggested theoretically for these hydrides. The periodic trends of physical properties of metal hydrides are discussed, based on the results reported in this and other recent studies.

1. Introduction

Recently, Marenich and Boggs[1] have investigated the Jahn−Teller distortion in SCH_3 using second-order multiconfiguration quasidegenerate perturbation theory (MCQDPT2), with explicit consideration of spin−orbit coupling effects. They concluded that Jahn−Teller distortion does not occur in the ground state (^{2}E) of SCH_3 (C_{3v}) when spin−orbit coupling (SOC) is included in the calculation, even though such a distortion is predicted to occur in the absence of SOC (Ham effect). This is an example of the importance of SOC effects in reliably describing the behavior of compounds that contain heavier elements. However, although there are many theoretical studies[2] of heavy metal compounds, most of these employed simple density functional theory (DFT), with few explicit investigations of relativistic effects. The use of relativistic effective core potentials[3−5] does not facilitate straightforward analysis of the role played by SOC. It still appears to be difficult to explicitly consider SOC effects in geometry optimizations of heavy metal compounds.

Spin−orbit coupling effects can also play an important role in describing transitions to electronically excited states.[6] SOC can induce intersystem crossing (ISC), for example, from an excited singlet state to low-lying triplet states and can also facilitate phosphorescence emitted by the transition from a triplet state to the ground singlet state. Similarly, nonadiabatic vibronic (derivative) coupling (NVC) is a key factor in nonradiative transitions among states possessing the same multiplicity. Thus, SOC and NVC play important roles in spectroscopy and photochemistry and it is therefore an important goal to treat these nonadiabatic interactions accurately to provide an adequate treatment of the behavior of electronically excited states.[7] For example, the results of a study of the emission rate of phosphorescence in heavy metal complexes will appear shortly.[8]

In recent years, several methods for predicting SOC effects in molecules have been developed[9−18] and implemented.[19−21] The current focus is on the importance of SOC effects in monohydrides of transition elements. Dissociation potential energy curves have been reported for group 3, 4, and 5 hydrides with use of multiconfiguration self-consistent-field (MCSCF) wave functions augmented by second-order configuration interaction (SOCI) calculations.[22,23] Those results are in good agreement with previously reported experimental and theoretical results. The present paper considers the hydrides of groups 6 and 7, in particular, the dissociation energy curves and SOC effects in low-lying electronic states of CrH, MoH, and WH, and MnH, TcH, and ReH. The tungsten hydrides are used in hydride-transfer reactions,[24,25] while chromium and molybdenum hydrides have been characterized in matrix isolation experiments.[26,27] Direct experimental characterization of neutral Re hydrides appears to be very difficult, while there are many reports on the corresponding anionic compounds.[28] There are several reports on manganese hydrides, but the structure of MnH_2 appears to be unclear.[29] Only a few papers can be found on technetium hydrides.[30−33] Since Tc is created artificially and

* To whom correspondence should be addressed. E-mail: shiro@c.s.osakafu-u.ac.jp, mark@si.fi.ameslab.gov.
† Osaka Prefecture University.
‡ Chisso Corporation.
§ Iowa State University.

10.1021/jp056258z CCC: $33.50
Published on Web 01/27/2006

TABLE 1: Spectroscopic Parameters for the Lowest Spin-Mixed States in Group 5 Hydrides[a]

mol.	state	method	R_e [Å]	D_e [cm^{-1}]	ω_e [cm^{-1}]	$\omega_e x_e$ [cm^{-1}]	B_e [cm^{-1}]	α_e [cm^{-1}]
VH	$\Omega = 0^+$	MCSCF	1.779	12493	1506	31.0	5.401	0.252
		FOCI	1.716	15601	1580	22.3	5.778	0.251
		SOCI	1.758	14766	1629	31.2	5.576	0.237
		expt[b]		17996 ± 565				
NbH	$\Omega = 0^+$	MCSCF	1.814	18052	1616	26.9	5.122	0.211
		FOCI	1.799	20118	1630	23.3	5.199	0.203
		SOCI	1.808	19811	1607	22.3	5.102	0.202
TaH	$\Omega = 2$	MCSCF	1.789	14187	1703	30.1	5.234	0.220
		FOCI	1.779	16083	1721	31.2	5.287	0.225
		SOCI	1.762	17002	1751	25.9	5.403	0.223
	$\Omega = 2$	AIMP[c]	1.762	22741				
	$\Omega = 0^+$	RECP[d]	1.775		1851			

[a] See the equation in the text. [b] Reference 43. They reported $D_0 = 2.13 \pm 0.07$ [eV] $= 17181 \pm 565$ [cm^{-1}]. The ω_e (SOCI) is used to obtain D_e. [c] Reference 44. [d] Reference 45.

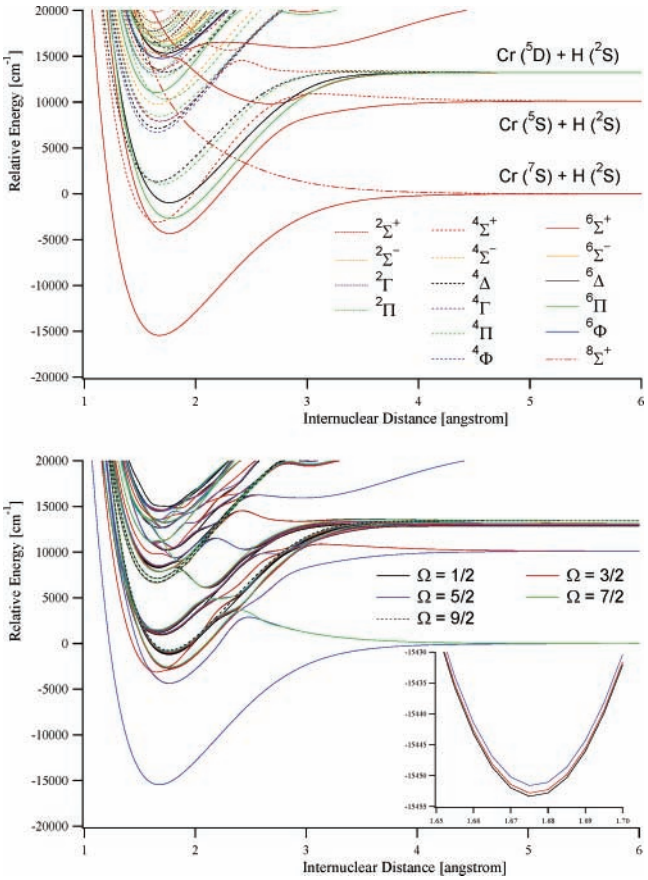

Figure 1. Potential energy curves for low-lying states in CrH. Top: Adiabatic curves. Bottom: Relativistic curves.

several Tc isotopes are radiatively stable, it is difficult to accurately characterize its chemical properties, although it is well-known that Tc easily forms many kinds of metal complexes.

The next section describes the computational methods used in the present investigation. The SOC effects on the properties of group 6 hydrides are discussed in Section 3. Then, after the discussion of group 7 hydrides, periodic trends in the physical properties of group 3, 4, 5, 6, and 7 hydrides are considered. All calculations have been performed with use of the GAMESS suite of program codes.[19−21]

2. Methods of Calculation

Effective core potential (ECP) calculations were carried out with multiconfiguration self-consistent-field (MCSCF) wave functions[34,35] followed by first-order configuration interaction (FOCI) calculations.[36] The SBKJC basis set[5] was employed in these calculations, augmented by a set of *f* functions[37] for transition elements and the 31G basis set augmented by a set of *p* functions for hydrogen.[38] The MCSCF active space will be described for each hydride in the following sections.

The MCSCF optimized orbitals were employed in FOCI calculations to construct SOC matrixes, where these matrix elements were computed by using the one-electron (Z_{eff}) approximation.[39] When ECP basis sets are used, the full Breit−Pauli Hamitonian leads to artificially small SOC splittings. This is caused by the neglect of core orbitals. Therefore, the present study examines the reliability of the one-electron approximation in order to apply it to large organometallic compounds. To keep the size of the matrixes computationally tractable, an energy tolerance (200−300 mhartree) was set for the excitation energy. All states within this energy range are included in the matrixes, so that the number of states varies slightly for each molecule.[40] For each molecule, the ground state within the LS coupling scheme and the lowest spin-mixed states are presented in the tables discussed below. In these tables Ω indicates the *z* component of the total angular momentum quantum number.

The equilibrium distances (R_e) were determined by fitting to a parabolic function near the energy minimum of each state. The dissociation energies (D_e) were defined by the difference between the energy in the dissociation limit and the minimum energy at R_e. The wave functions of the vibrational levels in each state are computed by using the discrete variable representation (DVR) method[41] and employed to compute the harmonic frequencies (ω_e), anharmonicities ($\omega_e x_e$), and rotational constants (B_e and α_e) for low-lying spin-mixed states. Then, the energy of a rovibrational state with vibrational v and rotational J quantum numbers in a given spin-mixed state is written as

$$E(v,J) = E_e + G(v) + F_v(J)$$
$$= E_e + \omega_e\left(v + \frac{1}{2}\right) - \omega_e x_e\left(v + \frac{1}{2}\right)^2 + \left\{B_e - \alpha_e\left(v + \frac{1}{2}\right)\right\}J(J+1)$$

where E_e is the electronic energy and the vibrational and rotational energies are approximated by $G(v) = \omega_e(v + {}^1/_2) - \omega_e x_e(v + {}^1/_2)^2$, and $F_v(J) = \{B_e - \alpha_e(v + {}^1/_2)\}J(J+1)$ in the present study. The electronic transition energies (T_e) were calculated as the difference between the minimum energies of two electronic states, while the 0−0 transition energy is the difference between the lowest vibrational levels of two electronic states.

TABLE 2: Spectroscopic Parameters for Low-lying CrH States

T_e [cm^{-1}]		R_e [Å]	D_e [cm^{-1}]	ω_e [cm^{-1}]	$\omega_e x_e$ [cm^{-1}]	B_e [cm^{-1}]	α_e [cm^{-1}]	μ^a [au]	ref
$X^6\Sigma^+$	0	1.676	15442	1616	35.2	6.033	0.300	4.190	
$A^6\Sigma^+$	11104	1.766	14443	1587	28.8	5.450	0.235	3.130	
$a^4\Sigma^+$	12439	1.658	13209	1783	36.5	6.206	0.283	3.010	
$B^6\Pi$	12749	1.770	15897	1588	30.5	5.417	0.240	3.065	
$C^6\Delta$	14433	1.763	14186	1535	30.6	5.457	0.251	3.042	
$\Omega = {}^1/_2$	0	1.676	15443	1616	35.2	6.033	0.300	4.189	
$\Omega = {}^3/_2$	1	1.676	15443	1616	35.2	6.033	0.300	4.189	
$\Omega = {}^5/_2$	2	1.676	15442	1616	35.2	6.033	0.300	4.190	
$\Omega = {}^1/_2$	11077	1.762	4362	1889	189.7	6.445	1.159	3.131	
$\Omega = {}^3/_2$	11082	1.762	4357	1889	189.9	6.445	1.159	3.130	
$\Omega = {}^5/_2$	11101	1.766	4332	1935	199.9	6.339	1.142	3.130	
$\Omega = {}^3/_2$	12295	1.647	13246	1530	27.2	5.789	0.326	3.010	
$\Omega = {}^1/_2$	12308	1.648	13263	1554	31.0	5.803	0.330	3.010	
$X^6\Sigma^+$			16376 ± 565						43
$X^6\Sigma^+$ (exptl)	0	1.655	16376 ± 565	1656	30.49	6.222	0.181		47
$X^6\Sigma^+$ (calcd)	0	1.654	18331	1654	31.0	6.132			47
$A^6\Sigma^+$ (exptl)	11616	1.786		1525	22.28	5.343	0.141		47
$A^6\Sigma^+$ (calcd)	10758−11270	1.765		1525	23.0	5.272			47
$X^6\Sigma^+$	0					6.132			51
$A^6\Sigma^+$	11553					5.272			51
$a^4\Sigma^+$	11186	1.672				6.10			
$X^6\Sigma^+$	0					6.127			57
$A^6\Sigma^+$	11553					5.269			57
$X^6\Sigma^+$		1.654	18887	1637					58
		1.662	15564	1587					58
		1.694	17173	1647					58

[a] Dipole moment calculated at the energy minimum of the lowest spin-mixed state.

3. Results and Discussion

3.1. Comparison of FOCI and SOCI Results. The second-order configuration interaction (SOCI) method was used in previous investigations to include the effects of external correlation in the hydrides of groups 3, 4, and 5.[42] In that study, to keep the computational effort tractable, only 13 external orbitals were used in the SOCI calculations of group 5 hydrides.[23] These 13 external orbitals are the lowest eigenvectors of the standard MCSCF Fock operator; they correlate with the n and $(n + 1)$sp orbitals for the transition element and with the 2sp orbitals for hydrogen in the dissociation limit. In such computations, it is generally difficult to choose an appropriate set of 13 external orbitals, especially in the bonding region of hydrides, because of strong interaction among the atomic orbitals. To avoid this somewhat artificial selection process, the present work employs the FOCI method. To calibrate this approach, the spectroscopic parameters for the group 5 hydrides were obtained by using MCSCF, FOCI, and selected SOCI wave functions for the spin−orbit coupling matrixes (see Table 1). In VH and NbH, FOCI predicts shorter R_e and larger D_e than does the selected SOCI, while this trend is reversed for TaH. In general, the properties predicted by FOCI are sufficiently close to the corresponding SOCI values that one expects the former method to be reasonably reliable. On the basis of the values presented in Table 1, the lanthanide contraction appears to be underestimated by the FOCI calculations. Unfortunately, no experimental data are available for NbH and TaH. Additionally, a disagreement has been found: the present study provided the ground state has $\Omega = 2$ originating from the lowest $^3\Phi$ state for TaH, and Wittborn and Wahlgren[44] also reported the ground state of $^3\Phi$ in TaH. On the other hand, Cheng and Balasubramanian[45] obtained the lowest $\Omega = 0^+$ state as the ground state in TaH (see Table 1 and Part II[23]).

3.2. CrH Potential Energy Curves. According to Moore,[46] the ground state correlates with a nondegenerate state [Cr (^{7}S) + H(^{2}S)] in the dissociation limit, where the Cr atom has the electronic configuration $(3d)^5\,(4s)^1$. The initial MCSCF active space used for this system includes the 10 orbitals that correlate with the 3d and 4sp orbitals of Cr and the 1s orbital of H in the dissociation limit, and the corresponding electrons. However, this "dsp" active space predicts ^{5}D as the ground state of Cr atom in the dissociation limit at the MCSCF level of theory. When the dynamic correlation effects are included by using the FOCI calculation, the lowest ^{7}S state becomes lower in energy than the ^{5}D state. Then, this result is consistent with experiment.[46] However, it should not be reasonable that the orbitals optimized for the lowest ^{5}D state are used to calculate potential energy curves correlating with the ^{7}S state. When the orbitals are optimized for the ^{7}S, the "dsp" active space is broken during MCSCF iteration: the pπ orbitals are replaced by outer dπ orbitals. Further investigations reveal that the MCSCF active space should include the 13 orbitals that are the lowest eigenvectors of the standard MCSCF Fock operator and that correlate with the 3d, 4s, 4d, and 5s orbitals of Cr and the H 1s orbital in the dissociation limit. This larger "dsds" active space correctly predicts Cr (^{7}S) + H (^{2}S) to be the ground state in the dissociation limit even within the MCSCF level of theory. The "dsds" space previously provided reasonable results for NbH.[23] In the present investigation, the MCSCF orbitals were optimized only for the ground state of CrH.

The MCSCF+FOCI adiabatic potential energy curves for the low-lying electronic states are plotted at the top of Figure 1. This figure shows that the ground state ($X^6\Sigma^+$) correlates with the ground state [Cr (^{7}S) + H(^{2}S)] in the dissociation limit, as mentioned above. The ground state in the dissociation limit also correlates with the lowest adiabatic repulsive $^8\Sigma^+$ state. The first excited state in the dissociation limit is Cr (^{5}S) + H (^{2}S), in which the Cr atom also has the electronic configuration $(3d)^5(4s)^1$. This state correlates with two bound states, $a^4\Sigma^+$ and $A^6\Sigma^+$ in the bonding region. The second excited-state Cr (^{5}D) + H (^{2}S) in the dissociation limit has the electronic configuration $(3d)^4\,(4s)^2$. This state splits into $^4\Sigma^+ + {}^4\Pi + {}^4\Delta$ and $^6\Sigma^+ + {}^6\Pi + {}^6\Delta$ in the bonding region of this hydride.

The potential energy curves that include relativistic effects are plotted at the bottom of Figure 1. The ground state has $\Omega = {}^1/_2$, where Ω is the z component of the total angular

TABLE 3: Electronic Excitation Energies and Transition Dipole Moments in Group 6 Hydrides

	transition	0−0 [cm^{-1}]	μ_{TM} [au]	ref
CrH	$X^6\Sigma_{1/2}^+-A^6\Sigma_{1/2}^+$	11077	1.41	
		11553	1.47	47, 51, 57
	$X^6\Sigma_{1/2}^+-B^6\Pi_{1/2}$	13077	0.55	
	$X^6\Sigma_{1/2}^+-B^6\Pi_{3/2}$	13104	0.58	
	$X^6\Sigma_{3/2}^+-A^6\Sigma_{3/2}^+$	11081	1.41	
	$X^6\Sigma_{3/2}^+-B^6\Pi_{1/2}$	12712	0.54	
	$X^6\Sigma_{3/2}^+-B^6\Pi_{5/2}$	12811	0.60	
	$X^6\Sigma_{5/2}^+-A^6\Sigma_{5/2}^+$	11099	1.42	
	$X^6\Sigma_{5/2}^+-B^6\Pi_{3/2}$	12724	0.58	
	$X^6\Sigma_{5/2}^+-B^6\Pi_{7/2}$	12854	0.60	
MoH	$X^6\Sigma_{1/2}^+-A^6\Sigma_{1/2}^+$	15590	1.69	
	$X^6\Sigma_{1/2}^+-c^4\Pi_{1/2}$	16056	< 0.1	
	$X^6\Sigma_{1/2}^+-B^6\Pi_{1/2}$	17697	0.84	
	$X^6\Sigma_{1/2}^+-B^6\Pi_{3/2}$	17772	0.59	
	$X^6\Sigma_{3/2}^+-A^6\Sigma_{3/2}^+$	15719	1.68	
	$X^6\Sigma_{3/2}^+-c^4\Pi_{3/2}$	16504	0.22	
	$X^6\Sigma_{3/2}^+-B^6\Pi_{1/2}$	17567	0.58	
	$X^6\Sigma_{3/2}^+-B^6\Pi_{3/2}$	17766	0.21	
	$X^6\Sigma_{3/2}^+-B^6\Pi_{5/2}$	17849	0.59	
	$X^6\Sigma_{5/2}^+-A^6\Sigma_{5/2}^+$	15808	1.49	
	$X^6\Sigma_{5/2}^+-c^4\Pi_{5/2}$	16618	0.30	
	$X^6\Sigma_{5/2}^+-B^6\Pi_{3/2}$	17467	0.61	
	$X^6\Sigma_{5/2}^+-B^6\Pi_{7/2}$	17890	0.59	
WH	$X^6\Sigma_{1/2}^+-A^6\Pi_{1/2}$	9401	0.53	
	$X^6\Sigma_{1/2}^+-A^6\Pi_{3/2}$	10262	0.41	
	$X^6\Sigma_{1/2}^+-B^6\Delta_{1/2}$	11919	0.20	
	$X^6\Sigma_{1/2}^+-c^4\Sigma_{1/2}^+$	13563	< 0.10	
	$X^6\Sigma_{1/2}^+-B^6\Pi_{3/2}$	13485	0.40	
	$X^6\Sigma_{1/2}^+-C^6\Sigma_{1/2}^+$	17464	0.87	
	$X^6\Sigma_{3/2}^+-c^4\Pi_{1/2}$	7676	0.26	
	$X^6\Sigma_{3/2}^+-A^6\Pi_{1/2}$	9242	0.37	
	$X^6\Sigma_{3/2}^+-A^6\Pi_{3/2}$	10103	0.20	
	$X^6\Sigma_{3/2}^+-A^6\Pi_{5/2}$	11194	0.23	
	$X^6\Sigma_{3/2}^+-B^6\Delta_{1/2}$	11760	0.54	
	$X^6\Sigma_{3/2}^+-B^6\Delta_{5/2}$	13809	0.33	
	$X^6\Sigma_{5/2}^+-A^6\Pi_{3/2}$	9872	0.43	
	$X^6\Sigma_{5/2}^+-A^6\Pi_{3/2}$	10305	0.38	
	$X^6\Sigma_{5/2}^+-A^6\Pi_{7/2}$	11742	0.69	
	$X^6\Sigma_{5/2}^+-B^6\Delta_{7/2}$	13881	0.25	

momentum quantum number (see the insert in Figure 1). Since the SOC is rather weak, the energy gaps among the levels are negligibly small and the spin-mixed states are quasidegenerate in energy, even though the adiabatic ground state ($X^6\Sigma^+$) is split into $\Omega = {}^1/_2$, $\Omega = {}^3/_2$, and $\Omega = {}^5/_2$ states by the SOC effects. It is not surprising that the SOC effects are small in hydrides of first-row transition elements. As a result, the inclusion of the SOC effects has a very small impact on the predicted spectroscopic parameters in these low-lying spin-mixed states (see Table 2).

Many reports on CrH can be found in the literature.[43,47−56] Table 2 includes the calculated and experimental results reported during the past decade, together with the present results. The latest study was carried out by Shin et al.[57] They observed the emission spectrum of the $A^6\Sigma^+-X^6\Sigma^+$ transition and analyzed the results to obtain the spectroscopic parameters for both electronic states. As shown in Table 2, the present estimations of the spectroscopic parameters seem reasonable in comparison with the corresponding observations, except that the dissociation energy is a bit too low. The $A^6\Sigma^+-X^6\Sigma^+$ 0−0 adiabatic transition energy is predicted to be 11 104 cm^{-1}, and after the inclusion of the spin−orbit coupling effects, the energy of the corresponding $A^6\Sigma_{1/2}^+-X^6\Sigma_{1/2}^+$ transition becomes slightly smaller (11 077 cm^{-1}; see Table 3). Since the experimental

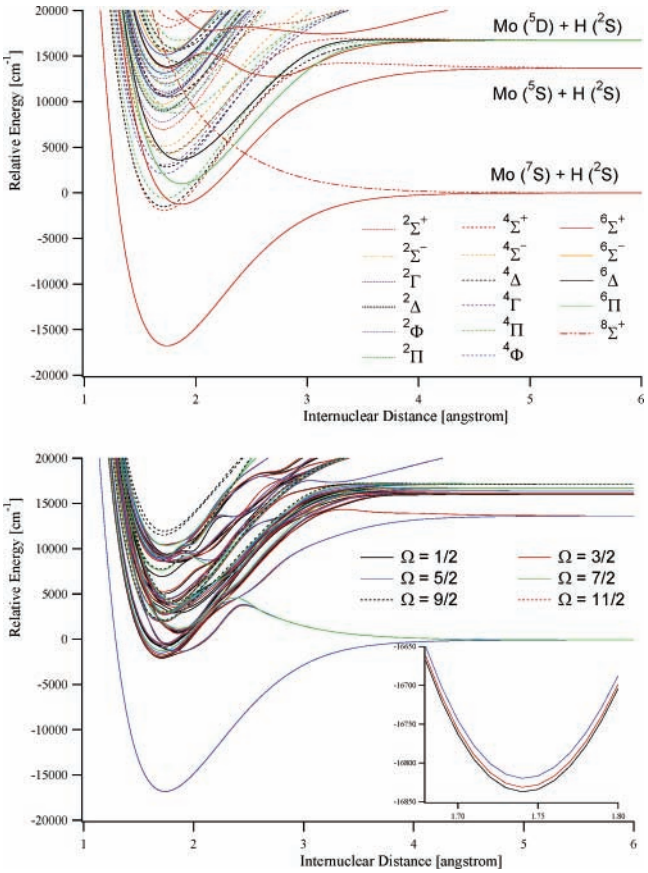

Figure 2. Potential energy curves for low-lying states in MoH. Top: Adiabatic curves. Bottom: Relativistic curves.

observation is reported to be 11 553 cm^{-1}, our method underestimates it by about 500 cm^{-1}. The transition dipole moment connecting the spin-mixed states $X^6\Sigma_{1/2}^+$ and $A^6\Sigma_{1/2}^+$ is calculated to be 0.77 au at the energy minimum of $A^6\Sigma_{1/2}^+$. Since $^6\Sigma_{1/2}^+$ states have two spin substates, the moments are multiplied by a factor of 2 (see Table 3). Bauschlicher et al.[47] report that the adiabatic transition moment for $A^6\Sigma^+-X^6\Sigma^+$ is in the range 0.70−0.73 au, so that the present results are reasonable. In addition, the present calculations suggest that a relatively weak emission (μ_{TM} = 0.28 au) corresponding to $B^6\Pi-X^6\Sigma^+$ appears near the transition energy of 13 000 cm^{-1} and a very strong emission (μ_{TM} = 1.48 au) of $D^6\Pi-X^6\Sigma^+$ near the transition energy of 26 500 cm^{-1} (not shown in the table because of its large transition energy).

3.3. MoH Potential Energy Curves. The ground state of Mo is ^{7}S, the same as Cr. The low-lying electronic states in the dissociation limit cannot be described correctly by using the "dsp" active space,[59] which is similar to CrH. Therefore, the "dsds" space was used in the MCSCF calculations; the MCSCF orbitals were optimized only for the ground state.

The MCSCF+FOCI adiabatic potential energy curves of the low-lying electronic states are plotted at the top of Figure 2. The results are similar to those discussed above for CrH: the ground state ($X^6\Sigma^+$) correlates with Mo (^{7}S) + H (^{2}S) in the dissociation limit, where Mo has the electronic configuration $(4d)^5(5s)^1$. The repulsive lowest $^8\Sigma^+$ state also correlates with Mo (^{7}S) + H (^{2}S) in the dissociation limit.

Moore[46] observed excitation energies of 7 593 and 10 768 cm^{-1} for the transitions from the ground state ^{7}S to the first excited state ^{5}S in Cr and Mo, respectively. The present calculations predict 10 119 and 13 690 cm^{-1} for these transitions, overestimated by 2500−2900 cm^{-1}. This disagreement

TABLE 4: Spectroscopic Parameters for Low-Lying MoH States

	T_e [cm^{-1}]	R_e [Å]	D_e [cm^{-1}]	ω_e [cm^{-1}]	$\omega_e x_e$ [cm^{-1}]	B_e [cm^{-1}]	α_e [cm^{-1}]	μ^a [au]	ref
$X^6\Sigma^+$	0	1.741	16757	1676	32.09	5.552	0.251	−4.059	
$a^4\Sigma^+$	14861	1.716	15653	1774	30.18	5.721	0.241	−3.657	
$b^4\Sigma^+$	15277	1.712	18255	1742	29.50	5.740	0.245	−3.951	
$A^6\Sigma^+$	15406	1.867	14948	1483	24.20	4.840	0.202	−2.745	
$c^4\Pi$	16186	1.725	17342	1731	28.99	5.655	0.239	−3.837	
$B^6\Pi$	17674	1.872	15731	1486	23.36	4.804	0.196	−2.741	
$d^4\Phi$	18882	1.716	19427	1735	31.46	5.710	0.250	−3.971	
$\Omega = {}^1/_2$	0	1.741	16764	1676	32.06	5.552	0.250	−4.057	
$\Omega = {}^3/_2$	6	1.741	16758	1675	32.07	5.551	0.250	−4.058	
$\Omega = {}^5/_2$	17	1.741	16747	1675	32.07	5.551	0.251	−4.059	
$\Omega = {}^1/_2$	14663	1.709	2023	1218	145.21	5.218	1.004	−3.652	
$\Omega = {}^3/_2$	14731	1.708	1944	1183	141.54	5.202	1.000	−3.651	
$\Omega = {}^1/_2$	14915	1.705	15546	1805	73.58	5.868	0.384	−3.928	
$\Omega = {}^3/_2$	15082	1.706	15363	1756	69.56	5.832	0.378	−3.941	
$\Omega = {}^5/_2$	15083	1.700	1460	941	112.62	3.667	0.496	−3.953	
$\Omega = {}^7/_2$	repulsive							−3.964	
$X^6\Sigma^+$		1.75	17628						30
$X^6\Sigma^+$		1.747	18149	1701					31
		1.746	17665	1642					31
			18552						31
$X^6\Sigma^+$				1675, 1727	26.0				60
$X^6\Sigma^+_{1/2}$	0	1.68	19601	1807					61
$X^6\Sigma^+_{3/2}$	118	1.68	19440	1808					61
$X^6\Sigma^+_{5/2}$	177	1.68	19440	1802					61
$b^4\Delta$	12033	1.65	18068	1846					61
$c^4\Pi$	14443	1.66	15648	1872					61
$B^6\Pi$	14494	1.79	15568	1604					61
$X^6\Sigma^+$				1720 ± 20					62

[a] See the footnote of Table 2.

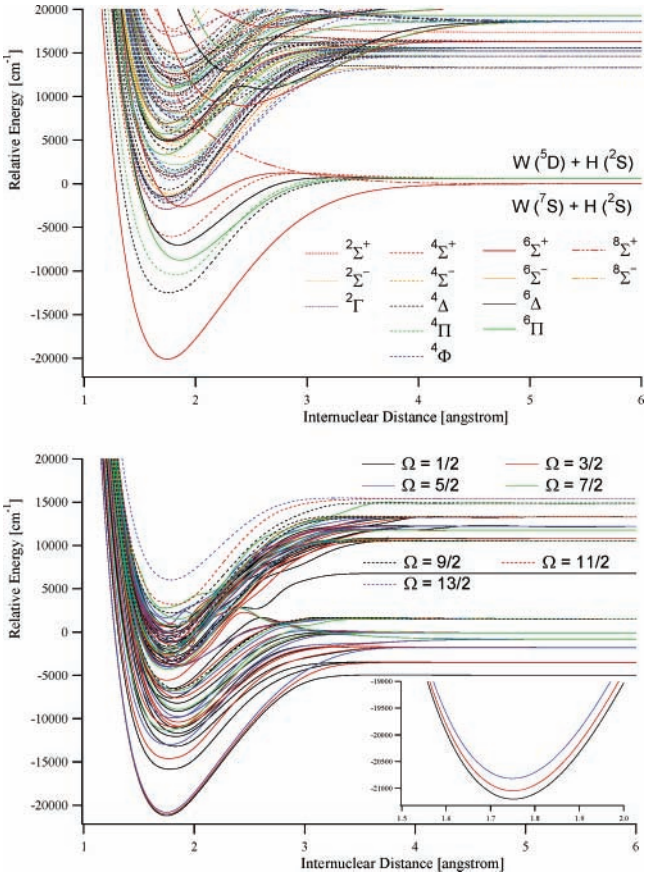

Figure 3. Potential energy curves for low-lying states in WH. Top: Adiabatic curves. Bottom: Relativistic curves.

is probably caused by the underestimation of dynamic correlation effects, due to the use of FOCI, instead of SOCI wave functions. The magnitude of the overestimation decreases dramatically, to less than 500 cm^{-1}, when SOCI wave functions are used for atomic Cr and Mo (8 025 and 11 231 cm^{-1}, respectively). Unfortunately, it is presently too time-consuming to carry out the SOCI calculations for these molecules.

To our knowledge, no paper was published on MoH during the past decade, but very recently Wang and Agdrews reported vibrational frequency for the ground state in MoH.[62] Their result and Siegbahn's results reported in 1993[30] are listed in Table 4, together with the present results. In some cases a range of values is given for the previous results. The present results are in these specific ranges and are therefore in reasonable agreement.

The most interesting result for this molecule is a potential surface crossing between the lowest excited sextet state $A^6\Sigma^+$ and some low-lying quartet states near the energy minimum of the $A^6\Sigma^+$ state. When the SOC effects are considered, the spin-mixed states that have the same Ω (*z*-component of the total angular momentum quantum number) avoid crossing of their potential energy curves near the energy minimum. As a result, the emission spectra of the $A^6\Sigma^+ - X^6\Sigma^+$ transition becomes rather broad. There does not appear to be a report on this emission spectrum, perhaps due to the complicated potential curves of the low-lying excited spin-mixed states near the energy minimum. Table 3 lists the relatively large dipole moments for the transitions between the ground state and low-lying excited states.

3.4. Potential Energy Curves in WH. Moore[45] reported that W has a $^5D_0$ ground state, below $^7S_3$ by only about 3000 cm^{-1}; both ^{5}D and ^{7}S states of W have $(5d)^5(6s)^1$ as the main electronic configuration. The adiabatic states, correlating with the lowest ^{5}D and ^{7}S states of W, must be very close in energy in the range of large internuclear distance. Therefore, the state-averaged MCSCF calculations include the lowest two $^6\Sigma^+$, one $^6\Pi$, and one $^6\Delta$ states with equal weights, where these states correlate with both W (^{5}D) + H (^{2}S) and W (^{7}S) + H (^{2}S) in the dissociation limit. The MCSCF active space includes the orbitals that correlate with the 5d and 6sp orbitals of W and the 1s orbital of H in the dissociation limit.

TABLE 5: Spectroscopic Parameters for Low-lying WH States

T_e [cm^{-1}]		R_e [Å]	D_e [cm^{-1}]	ω_e [cm^{-1}]	$\omega_e x_e$ [cm^{-1}]	B_e [cm^{-1}]	α_e [cm^{-1}]	μ^a [au]	ref
$X^6\Sigma^+$	0	1.746	20108	1811	33.0	5.544	0.234	−3.957	
$a^4\Delta^+$	7457	1.754	13057	1494	8.9	5.449	0.238	−3.598	
$b^4\Pi^+$	9481	1.826	10981	1422	8.5	5.202	0.227	−3.271	
$A^6\Pi^+$	11208	1.865	9337	1507	41.9	4.859	0.256	−3.043	
$B^6\Delta$	12960	1.840	7604	1557	57.6	5.046	0.313	−3.072	
$c^4\Sigma^+$	13908	1.784	6654	1680	80.58	6.125	0.745	−3.791	
$^2\Sigma^+$	17105	1.735	18485	1680	15.80	5.575	0.224	−3.757	
$\Omega = {}^1/_2$	0	1.751	16224	1788	34.0	5.506	0.237	−3.920	
$\Omega = {}^3/_2$	159	1.750	17526	1793	33.5	5.514	0.236	−3.937	
$\Omega = {}^5/_2$	390	1.749	19036	1799	32.9	5.524	0.234	−3.959	
$\Omega = {}^1/_2$	5157	1.776	12319	1434	6.9	5.355	0.236	−3.502	
$\Omega = {}^3/_2$	6399	1.770	12831	1457	7.4	5.381	0.234	−3.533	
$\Omega = {}^1/_2$	7835	1.831	9678	1484	31.2	5.144	0.260	−3.213	
$\Omega = {}^5/_2$	8015	1.766	12199	1477	8.9	5.399	0.236	−3.570	
$\Omega = {}^1/_2$	8941	1.832	10283	1423	27.3	5.155	0.266	−3.237	
$\Omega = {}^1/_2$	9401	1.852	9889	1564	36.5	5.018	0.246	−3.197	
$\Omega = {}^7/_2$	9696	1.763	10533	1511	17.3	5.441	0.258	−3.597	
$\Omega = {}^1/_2$	9994	1.852	10281	1568	33.6	4.974	0.236	−3.117	
$\Omega = {}^3/_2$	10001	1.826	9164	1312	17.7	5.110	0.265	−3.281	
$\Omega = {}^3/_2$	10262	1.859	10062	1628	55.5	4.951	0.267	−3.094	
$\Omega = {}^3/_2$	10695	1.855	9591	1603	34.2	4.963	0.227	−3.076	
$\Omega = {}^5/_2$	11059	1.816	9092	1334	20.4	5.137	0.269	−3.316	
$\Omega = {}^5/_2$	11353	1.857	9702	1681	41.2	5.000	0.228	−3.071	
$X^6\Sigma^+$		1.720	24137						64
		1.725	23766						64
$X^6\Sigma^+$		1.71	22000	1820					65
		1.73	21685	1897					65
$X^6\Sigma^+$		1.79 ± 0.02		531 ± 62		5.21 ± 0.13			66
$A^6\Pi$		1.90 ± 0.02		409 ± 60		4.65 ± 0.11			66
$X^6\Sigma^+$		1.706		1934					67
				1860					

[a] See the footnote of Table 2.

As shown at the top of Figure 3, the ground state is $^6\Sigma^+$ (denoted $X^6\Sigma^+$) and correlates with the lowest state [W (^{7}S) + H (^{2}S)] in the dissociation limit within the MCSCF+FOCI adiabatic *ansatz*. Although W (^{5}D) + H (^{2}S) is the second lowest state in the dissociation limit at this level of theory, the energy difference between the lowest and second lowest states is calculated to be only 582 cm^{-1}, and the SOC splitting is expected to be larger than this difference. The ground state [W (^{7}S) + H (^{2}S)] in the dissociation limit also correlates with the repulsive lowest $^8\Sigma^+$ state.

For atomic W (in the dissociation limit of WH), the lowest ^{5}D state is split into ^{5}D$_0$, ^{5}D$_1$, ^{5}D$_2$, ^{5}D$_3$, and ^{5}D$_4$ by SOC, and Moore[45] has reported relative energies of 0 (^{5}D$_0$), 1670 (^{5}D$_1$), 2951 (^{7}S$_3$), 3326 (^{5}D$_2$), 4830 (^{5}D$_3$), and 6219 (^{5}D$_4$) cm^{-1} for these states. In the present study these values are predicted to be 0 (^{5}D$_0$), 1458 (^{5}D$_1$), 3196 (^{5}D$_2$), 4169 (^{7}S$_3$), 4897 (^{5}D$_3$), and 6512 (^{5}D$_4$) cm^{-1}.[63] The energy gap between the lowest ^{5}D$_0$ and ^{7}S$_3$ states is still overestimated by about 1200 cm^{-1},[64] but the energetic order of these states agrees with Moore's report. Thus, it is important to include the SOC effects to predict the correct dissociation limit.

The relativistic potential curves obtained after the inclusion of the SOC effects are plotted at the bottom of Figure 3. In the range of smaller internuclear distances, the ground state $X^6\Sigma^+$ is split into $\Omega = {}^1/_2$, ${}^3/_2$, and ${}^5/_2$. The ground state in the relativistic scheme has $\Omega = {}^1/_2(X^6\Sigma^+_{1/2})$. As shown in Table 5, the SOC effect makes the dissociation energy D_e of the ground state smaller by about 4000 cm^{-1} and its equilibrium internuclear distance R_e shorter by 0.005 Å. To our knowledge, there is no experimental report on the dissociation energy, while Garvey et al.[65,66] observed 1.79 Å for R_e. The latest theoretical calculation has been performed with use of the AREP+SOCI method with AIMP.[65] Their results are closer to the adiabatic values in Table 5.

Unfortunately, no paper on the emission spectra of WH was found. According to the present analysis (see Table 3), the electronic transitions $A^6\Pi-X^6\Sigma^+$ and $C^6\Sigma^+-X^6\Sigma^+$ are observed near 11 000 and 17 800 cm^{-1}, respectively. However, the corresponding transition dipole moments are calculated to be relatively small (μ_{TM} 0.47 au), so these transitions could be hidden by the tails of the strong transitions in the range of 25 000 cm^{-1}. Thus, no visibly large transition is obtained in the 10 000−20 000 cm^{-1} range in the present calculations. This suggests that it might be difficult to analyze the experimental spectra of WH.

3.5. Potential Energy Curves for Group 7 Hydrides: MnH, TcH, and ReH. The ground state in group 7 hydrides correlates with M (^{6}S) + H (^{2}S) (M = Mn, Tc, Re) in the dissociation limit, where the main electron configuration in the ground state of each transition element is $(n$d$)^5[(n+1)$s$]^2$ rather than $(n$d$)^6[(n+1)$s$]^1$ (n = 3, 4, 5). Since the ground state is not degenerate and the next lowest electronic state is rather higher in energy than the ground state in the dissociation limit,[46] the MCSCF orbitals are optimized only for the ground state in each hydride. The MCSCF active space includes the orbitals correlating with nd and (n+1)sp orbitals (n = 3, 4, 5) of the transition element and the 1s orbital of hydrogen. Several trials reveal that MnH has a septet ground state, while TcH and ReH have quintet ground states. Thus, the MCSCF orbitals have been optimized for the lowest $^7\Sigma^+$ state in MnH and for the lowest $^5\Sigma^+$ state in TcH and ReH.

The lowest $^7\Sigma^+$ and $^5\Sigma^+$ states in the group 7 hydrides become degenerate in the dissociation limit and correlate with the ground state M (^{6}S) + H (^{2}S) (M = Mn, Tc, or Re). In MnH, the lowest $^7\Sigma^+$ state becomes lower in energy than the lowest $^5\Sigma^+$ state as the internuclear distance decreases. As a result, the lowest $^7\Sigma^+$ state is the ground state near the energy minimum of MnH, so that this state should be denoted $X^7\Sigma^+$. On the other hand,

TABLE 6: Spectroscopic Parameters for Low-lying MnH, TcH, and ReH States

	T_e [cm^{-1}]		R_e [Å]	D_e [cm^{-1}]	ω_e [cm^{-1}]	$\omega_e x_e$ [cm^{-1}]	B_e [cm^{-1}]	α_e [cm^{-1}]	μ^a [au]	ref
MnH	$X^7\Sigma^+$	0	1.702	11741	1503	24.9	5.895	0.299	3.149	
	$a^5\Sigma^+$	4124	1.644	7624	1493	54.3	6.268	0.427	3.068	
	$b^5\Pi$	18341	1.563	16687	1662	21.8	6.847	0.332	4.018	
	$c^5\Sigma^+$	18532	1.583	16518	1689	32.7	6.719	0.359	3.910	
	$A^7\Pi$	20162	1.691	8301	1371	49.0	5.837	0.394	3.871	
	$\Omega = 0^+$	0	1.702	11741	1503	24.9	5.895	0.299	3.149	
	$\Omega = 1$	0	1.702	11769	1503	24.9	5.895	0.299	3.149	
	$\Omega = 2$	0	1.702	11741	1503	24.9	5.895	0.299	3.149	
	$\Omega = 3$	1	1.702	11740	1503	24.9	5.895	0.299	3.149	
	$\Omega = 0^+$	4123	1.644	7625	1493	54.3	6.268	0.427	3.068	
	$\Omega = 1$	4123	1.644	7625	1493	54.3	6.268	0.427	3.068	
	$\Omega = 2$	4124	1.644	7624	1493	54.3	6.268	0.427	3.067	
	$X^7\Sigma^+$	0			1542	27.9				29
			1.735		1507					29 (DFT)
	$a^5\Sigma^+$	6645	1.644		1605					29 (DFT)
	$X^7\Sigma^+$		1.723	8674	1542					58
			1.740	13640	1548					58
	$X^7\Sigma^+$	0	1.73							68
	$A^7\Pi$	28020								69
	$X^7\Sigma^+$		1.7309		1547		5.686			70
	$a^5\Sigma^+$		1.6246				6.453			71
			1.6252		1722	70	6.4491	0.192		70
	$b^5\Pi$		1.6320							70
	$c^5\Sigma^+$		1.6432				6.3082			71
	$d^5\Pi$		1.6569		1638		6.2045	0.1645		
	$e^5\Sigma^+$		1.7540		1660		5.5367*			
TcH	$X^5\Sigma^+$	0	1.677	12709	1764	40.5	6.000	0.299	−3.272	
	$a^7\Sigma^+$	1608	1.869	10917	1392	27.1	4.831	0.223	−2.585	
	$A^5\Pi$	5773	1.692	17037	1678	32.8	5.867	0.277	−3.698	
	$B^5\Delta$	7717	1.729	15047	1587	33.3	5.621	0.276	−3.832	
	$C^5\Sigma^+$	11880	1.837	10774	1370	34.0	4.997	0.266	−2.785	
	$b^7\Pi$	15006	1.696	7810	1723	52.4	6.782	0.812	−3.424	
	$\Omega = 0^+$	0	1.678	12748	1612	56.45	5.840	0.346	−3.277	
	$\Omega = 1$	17	1.678	12731	1608	56.01	5.836	0.345	−3.275	
	$\Omega = 2$	65	1.678	12681	1595	54.75	5.823	0.343	−3.272	
	$\Omega = 3$	1649	1.868	10925	1392	29.85	4.820	0.204	−2.607	
	$\Omega = 0^+$	1838	1.864	10980	1877	66.97	5.131	0.217	−2.590	
	$\Omega = 1$	1839	1.865	10982	1881	68.36	5.132	0.213	−2.592	
	$\Omega = 2$	1842	1.865	10987	1893	70.89	5.141	0.211	−2.598	
	$X^5\Sigma^+$		1.67	14795						30
	$X^5\Sigma^+$	0	1.704	16778	1841					31
	$a^7\Sigma^+$	1400	1.824	15245	1580					
	$X^5\Sigma^+$	0	1.671	15729	1797					31
	$a^7\Sigma^+$	1130	1.833	14600	1531					
	$a^7\Sigma^{+a}$	0	1.752	21214	1633					32
	$X^5\Sigma^{+a}$	2619	1.612	18633	1930					
	$A^5\Pi$	5208	1.611	22585	1811					
		1129								33
ReH	$X^5\Sigma^+$	0	1.662	12537	1959	53.9	6.104	0.321	3.249	
	$a^7\Sigma^+$	3415	1.842	8872	1457	39.7	4.966	0.276	2.877	
	$A^5\Pi$	10580	1.676	21327	1928	35.8	5.960	0.258	3.717	
	$B^5\Delta$	13615	1.692	18277	1903	38.7	5.853	0.263	3.710	
	$b^7\Pi$	15804	1.670	15061	1958	50.59	6.033	0.305	3.532	
	$C^5\Sigma^+$	15897	1.753	15892	1690	34.64	5.446	0.253	3.076	
	$^3\Sigma^-$	16026	1.653	17850	2024	42.1	6.140	0.277	3.568	
	$\Omega = 0^+$	0	1.663	12958	2000	70.3	6.154	0.366	3.263	
	$\Omega = 1$	306	1.664	12650	1997	76.2	6.138	0.374	3.259	
	$\Omega = 2$	823	1.666	12125	1976	83.7	6.096	0.384	3.240	
	$\Omega = 3$	3790	1.837	8920	1456	39.6	4.994	0.274	2.950	
	$\Omega = 2$	3914	1.836	8818	1602	38.1	5.125	0.266	2.917	
	$\Omega = 1$	3955	1.839	8765	1541	32.5	5.062	0.259	2.893	
	$\Omega = 0^+$	3964	1.841	8751	1501	28.4	5.023	0.253	2.885	
	$X^5\Sigma^+$	0	1.640		2102					29
	$a^7\Sigma^+$	7800	1.812		1560					29
	$X^5\Sigma^+$		1.640	18422						44
			1.640	18561						44
	$X^5\Sigma^+$		1.64	16159	1950					65
			1.63	7730	2042					65
	$a^7\Sigma^+$		1.79	12626	1550					65
			1.82	10633	1611					65

[a] They reported that the lowest state is $^7\Sigma^+$ (see ref 32).

TABLE 7: Electronic Excitation Energies and Transition Dipole Moments in Group 7 Hydrides

	transition	0−0 [cm^{-1}]	μ_{TM} [au]
MnH	$X^7\Sigma^+_{0+}-A^7\Pi_1$	20187	1.93
	$X^7\Sigma^+_1-A^7\Pi_{0^+}$	20174	1.36
	$X^7\Sigma^+_1-A^7\Pi_{0^-}$	20185	1.36
	$X^7\Sigma^+_1-A^7\Pi_2$	20176	2.72
	$X^7\Sigma^+_2-A^7\Pi_1$	20173	2.72
	$X^7\Sigma^+_2-A^7\Pi_3$	20175	2.72
	$X^7\Sigma^+_3-A^7\Pi_2$	20165	2.72
	$X^7\Sigma^+_3-A^7\Pi_4$	20166	2.72
TcH	$X^5\Sigma^+_{0+}-A^5\Pi_1$	5801	0.48
	$X^5\Sigma^+_{0+}-C^5\Sigma^+_{0+}$	11955	0.97
	$X^5\Sigma^+_1-A^5\Pi_2$	5638	0.66
	$X^5\Sigma^+_1-A^5\Pi_0$	5947	0.34
		5993	0.34
	$X^5\Sigma^+_1-C^7\Sigma^+_1$	11939	1.94
	$X^5\Sigma^+_2-A^5\Pi_3$	5492	0.66
	$X^5\Sigma^+_2-A^5\Pi_1$	6136	0.70
	$X^5\Sigma^+_2-C^5\Sigma^+_2$	11890	1.95
ReH	$X^5\Sigma^+_{0+}-A^5\Pi_1$	10904	0.41
	$X^5\Sigma^+_{0+}-A^5\Pi_{0^+}$	11315	0.16
	$X^5\Sigma^+_{0+}-A^5\Pi_{0^+}$	12712	0.19
	$X^5\Sigma^+_1-A^5\Pi_2$	9971	0.56
	$X^5\Sigma^+_1-A^5\Pi_1$	10598	0.33
	$X^5\Sigma^+_1-A^5\Pi_{0^+}$	11009	0.31
	$X^5\Sigma^+_1-A^5\Pi_{0^-}$	11560	0.31
	$X^5\Sigma^+_2-A^5\Pi_3$	9334	0.54
	$X^5\Sigma^+_2-A^5\Pi_2$	9454	0.26
	$X^5\Sigma^+_2-A^5\Pi_1$	11380	0.64

although the lowest $^7\Sigma^+$ state is lower in energy than the lowest $^5\Sigma^+$ state in the region of long internuclear distances, the potential energy curves of these states cross at $R \sim 1.917$ (TcH) or 2.062 Å (ReH). The lowest $^5\Sigma^+$ state becomes the ground state near the energy minima of TcH and ReH, so that it should be denoted by $X^5\Sigma^+$. In these three hydrides, the main configurations near the energy minima are

$$\text{core}(n\text{d}\sigma_{\text{bonding}})^2(n\text{d}\sigma_{\text{lone-pair}})^2(n\text{d}\pi)^2(n\text{d}\delta)^2$$

for the lowest $^5\Sigma^+$ state and

$$\text{core}(n\text{d}\sigma_{\text{bonding}})^2(n\text{d}\sigma_{\text{lone-pair}})^1(n\text{d}\pi)^2(n\text{d}\delta)^2(n\text{d}\sigma_{\text{antibonding}})^1$$

for the lowest state $^7\Sigma^+$. The discrepancy between MnH and TcH/ReH seems to be caused by the larger energy splitting between the 3d and 4s orbitals in atomic Mn in comparison with those between 4d and 5s orbitals in Tc and between the 5d and 6s orbitals in Re. In other words, the antibonding orbital $3\text{d}\sigma_{\text{antibonding}}$, which consists of Mn 3d_z^2 and 4s orbitals and the H 1s orbital, is closer in energy to the nonbonding orbitals $3\text{d}\sigma_{\text{lone-pair}}$, $3\text{d}\pi$, and $3\text{d}\delta$, in comparison with those in TcH and ReH. As a result, MnH has the ground state $X^7\Sigma^+$ generated by the excitation from $3\text{d}\sigma_{\text{lone-pair}}$ to $3\text{d}\sigma_{\text{antibonding}}$ near the equilibrium internuclear distance. The energy gap between $3\text{d}\sigma_{\text{lone-pair}}$ and $3\text{d}\sigma_{\text{antibonding}}$ is larger in TcH and ReH, so that the lowest $^5\Sigma^+$ state stays lower in energy than the lowest $^7\Sigma^+$ state.

Within the adiabatic picture, the energy gaps of the lowest $^7\Sigma^+$ and $^5\Sigma^+$ states are −4124 (MnH), 1608 (TcH), and 3415 (ReH) cm^{-1} at the equilibrium internuclear distances, respectively, where the negative value indicates that $^7\Sigma^+$ is lower in energy than $^5\Sigma^+$. After the inclusion of SOC effects, the energy gaps of the lowest $^7\Sigma^+_{0+}$ and $^5\Sigma^+_{0+}$ states are estimated to be −4123 (MnH), 1838 (TcH), and 3964 (ReH) cm^{-1}, respectively.

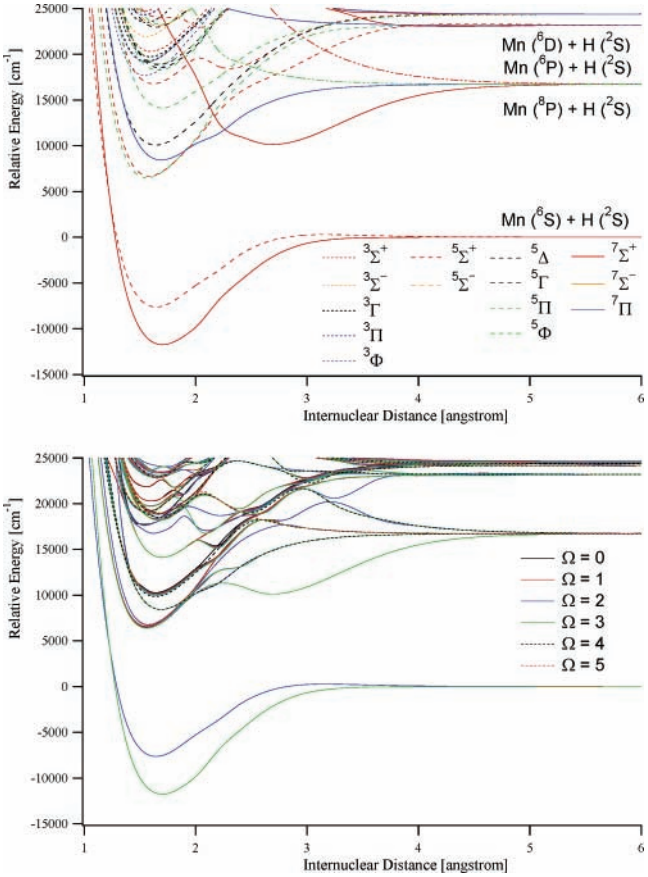

Figure 4. Potential energy curves for low-lying states in MnH. Top: Adiabatic curves. Bottom: Relativistic curves. The energetically lowest curve overlaps those for the lowest $\Omega = 0^+$, 1, 2, and 3 states, since the SOC splittings are negligibly small (see Table 6). The second lowest curve overlaps those for the second lowest $\Omega = 0^+$, 1, and 2 states. $\Omega = 0^+$ and 0^- are simplified as "0" in the figure.

The energy gaps increase in TcH and ReH because strong SOC occurs between the spin-mixed states with the same value of Ω. In fact, the spin-mixed states originating from $a^7\Sigma^+$ have an inverted order (Ω = 3, 2, 1, 0) in ReH (see Table 6), since larger coupling occurs in the states of smaller Ω. Because of the small energy gaps between the $a^7\Sigma^+_{0+}$ and $X^5\Sigma^+_{0+}$ states in TcH, the energetic order of these states is sensitive to the methods of calculation. In fact, although it has been reported[32] that the $a^7\Sigma^+$ state is lower in energy than the $X^5\Sigma^+$ state in TcH, more recent studies[30,31] have concluded that the ground state is $X^5\Sigma^+$. The latest study on MnH and ReH, by Wang and Andrews in 2003,[29] reports that the energy gaps of the lowest $^5\Sigma^+$ and $^7\Sigma^+$ states are −6645 (MnH) and 7800 (ReH) cm^{-1}, respectively. There is no recent experimental report on this gap in TcH. Balasubramanian[31] reported a gap of 1130 cm^{-1} using the MCPF method. The present results are in good qualitative agreement with these, though the gaps predicted here are somewhat larger.

Unfortunately, the order of the low-lying excited states in the dissociation limit of these hydrides is not consistent with Moore's experimental results for the atoms. The most likely origins of this discrepancy are that the MCSCF orbitals are optimized only for the ground state and the FOCI method is not sufficient to adequately estimate the effects of dynamic electron correlation for excited states. Nonetheless, the molecular emission spectra are discussed here on the basis of the present computational results. The spectral analysis of MnH has been achieved by Varberg et al.[68] They have reported that the

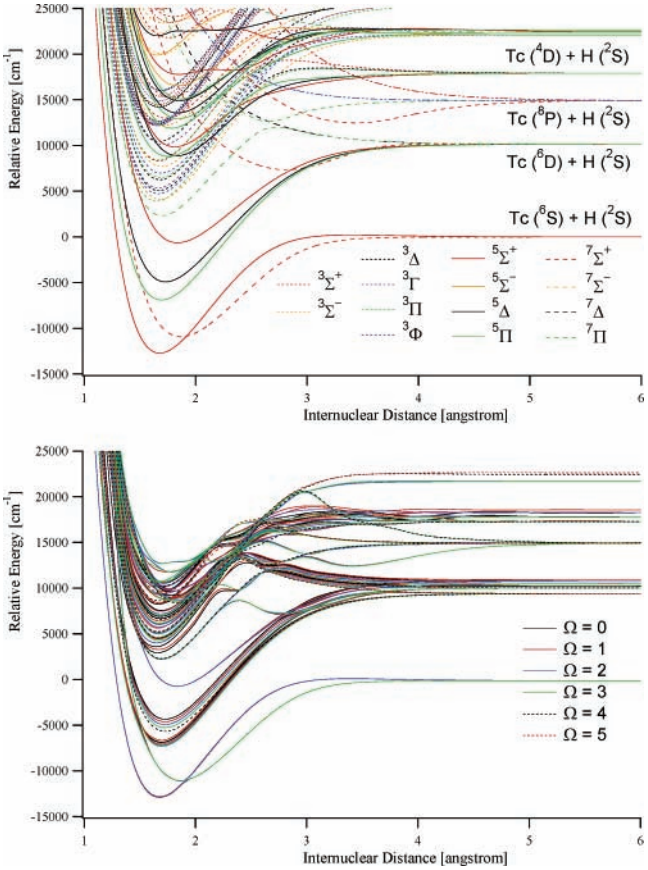

Figure 5. Potential energy curves for low-lying states in TcH. Top: Adiabatic curves. Bottom: Relativistic curves. The energetically lowest curve near the energy minimum overlaps those for the lowest $\Omega = 0^+$, 1, and 2 states, since the SOC splittings are relatively small (see Table 6). The second lowest curve also overlaps those for the second lowest $\Omega = 0^+$, 1, and 2 states and the lowest $\Omega = 3$ state. $\Omega = 0^+$ and 0^- are simplified as "0" in the figure.

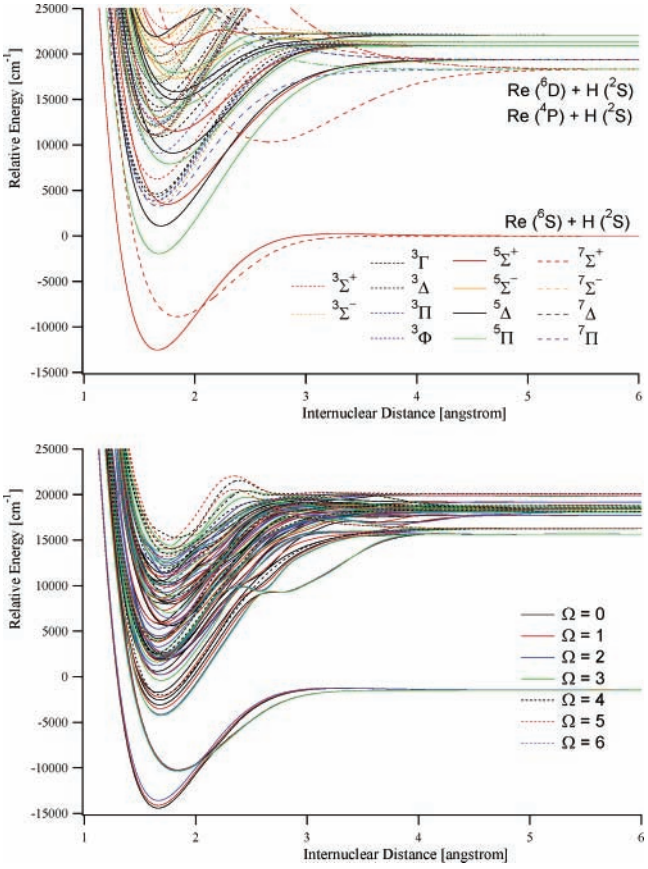

Figure 6. Potential energy curves for low-lying states in ReH. Top: Adiabatic curves. Bottom: Relativistic curves. The energetically lowest curve near the energy minimum overlaps those for the lowest $\Omega = 0^+$, 1, and 2 states, since the SOC splittings are relatively small (see Table 6). The second lowest curve also overlaps those for the second lowest $\Omega = 0^+$, 1, and 2 states and the lowest $\Omega = 3$ state. $\Omega = 0^+$ and 0^- are simplified as "0" in the figure.

emission $A^7\Pi-X^7\Sigma^+$ appears in the energy range of 17 500−18 000 cm^{-1}, while the present calculations provide a large transition moment for $A^7\Pi-X^7\Sigma^+$ near the transition energy of 20 000 cm^{-1} (see Table 7). So, the present transition energy is overestimated by about 10%.

Unfortunately, there does not appear to be any published work on the electronic spectrum of TcH. The present results suggest that the $C^5\Sigma^+-X^5\Sigma^+$ transition has a relatively large transition moment ($\mu_{TM} \approx 1$ au) and appears near 13 000 cm^{-1} (Table 7). In addition, a strong and broad transition corresponding to $D^5\Pi-X^5\Sigma^+$ is predicted near 22 000 cm^{-1} and the tail of this emission could hide the peak of the $C^5\Sigma^+-X^5\Sigma^+$ transition. Given the 10% overestimation noted above, these transition energies might need to be divided by a factor of 1.1. To our knowledge, there is also no report on the electronic spectra in ReH. The present calculations predict two peaks corresponding to $A^5\Pi-X^5\Sigma^+$ ($\mu_{TM} = 0.1-0.2$ au) and $C^5\Sigma^+-X^5\Sigma^+$ ($\mu_{TM} = 0.65$ au) near the transition energies of 11 000 and 16 000 cm^{-1}, respectively. The former is weaker than the latter.

3.6. Periodic Trends of Spectroscopic Parameters for the Ground States in Group 3−7 Hydrides. The previous paper[23] discussed the periodic trends of the spectroscopic parameters in groups 3, 4, and 5 hydrides. In this section, these trends are re-considered in view of the new results presented here for group 6 and 7 hydrides.

The hydride dissociation energies D_e, calculated for the lowest spin-mixed state by using the SBKJC(f,p) basis set, are plotted vs the group number of transition elements in Figure 7. As the

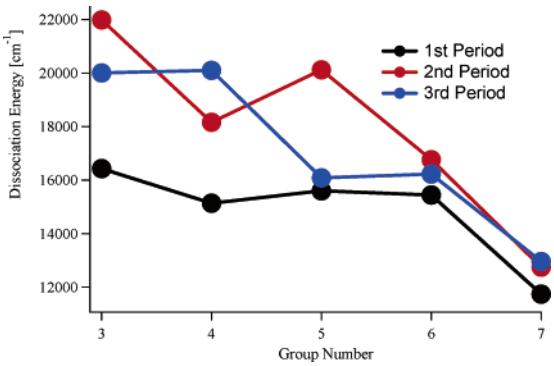

Figure 7. Dependence of hydride dissociation energies vs group number.

group number of transition elements increases from left to right across the periodic table, D_e tends to decrease, although not monotonically. As mentioned in the previous paper, this is caused by the increase in the screening of the nuclear charge by d electrons as their number increases. Since the screening is relatively weaker than that by sp electrons, the slope of the D_e line is expected to be smaller than that for main-group elements.

The equilibrium internuclear distance R_e in the lowest spin-mixed state vs the row number for transition elements is plotted in Figure 8. The trend for the group 3 hydrides, in which R_e monotonically increases with increasing row number, is apparently different from those for the other hydrides. This is mainly because the primary variation in group 3 is the expansion of

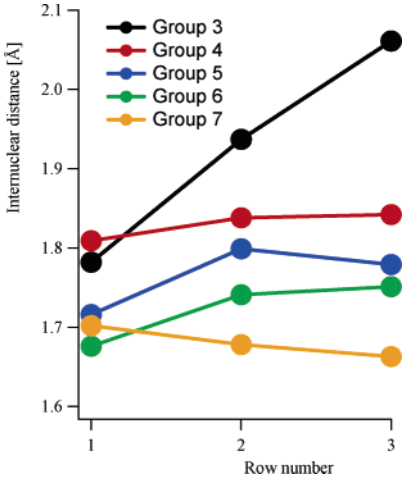

Figure 8. Dependence of equilibrium internuclear distances in the hydrides vs row number of the periodic table.

TABLE 8: Ground States in Atoms and the Corresponding Hydrides

	group 3	group 4	group 5	group 6	group 7
atoms					
row 1	Sc	Ti	V	Cr	Mn
	$^2D_{3/2}$	$^2F_3$	$^4F_{3/2}$	$^7S_3$	$^6S_{5/2}$
row 2	Y	Zr	Nb	Mo	Tc
	$^2D_{3/2}$	$^2F_3$	$^6D_{1/2}$	$^7S_3$	$^6S_{5/2}$
row 3	La	Hf	Ta	W	Re
	$^2D_{3/2}$	$^2F_3$	$^4F_{3/2}$	$^5D_0$	$^6S_{5/2}$
hydrides					
row 1	ScH	TiH	VH	CrH	MnH
	$^1\Sigma^+_{0^+}$	$^4\Phi_{2/3}$	$^5\Delta_{0^+}$	$^6\Sigma^+_{1/2}$	$^7\Sigma^+_{0^+}$
row 2	YH	ZrH	NbH	MoH	TcH
	$^1\Sigma^+_{0^+}$	$^2\Delta_{2/3}$	$^5\Delta_{0^+}$	$^6\Sigma^+_{1/2}$	$^5\Sigma^+_{0^+}$
row 3	LaH	HfH	TaH	WH	ReH
	$^1\Sigma^+_{0^+}$	$^2\Delta_{2/3}$	$^3\Phi_2$	$^6\Sigma^+_{1/2}$	$^5\Sigma^+_{0^+}$

the valence d orbitals as the principal quantum number increases. For the other groups, the screening of the 4f electrons in the third row is rather weak and the s orbitals contract while the d and f orbitals expand. Consequently, the attraction between the transition element and the hydrogen becomes larger. This is so-called "lanthanide contraction".

The ground states in group 3−7 hydrides are summarized in Table 8. The reason these ground states are obtained for these hydrides may be explained as follows: The energetic order of the valence orbitals is $nd\sigma_{bonding}$, $nd\sigma_{lone-pair}$, $nd\pi$, $nd\delta$, $nd\sigma_{antibonding}$. Therefore, the ground-state electronic configuration should be

$^1\Sigma^+$: core$(nd\sigma_{bonding})^2(nd\sigma_{lone-pair})^2$
for group 3 hydrides

$^2\Delta$: core$(nd\sigma_{bonding})^2(nd\sigma_{lone-pair})^2(nd\pi)^0(nd\delta)^1$
for group 4 hydrides

$^3\Phi$: core$(nd\sigma_{bonding})^2(nd\sigma_{lone-pair})^2(nd\pi)^1(nd\delta)^1$
for group 5 hydrides

$^6\Sigma^+$: core$(nd\sigma_{bonding})^2(nd\sigma_{lone-pair})^1(nd\pi)^2(nd\delta)^2$
for group 6 hydrides

$^5\Sigma^+$: core$(nd\sigma_{bonding})^2(nd\sigma_{lone-pair})^2(nd\pi)^2(nd\delta)^2$
for group 7 hydrides

However, as mentioned for group 7 hydrides, the $nd\sigma_{lone-pair}$ orbital is relatively higher in energy when the row number is small. This is the reason that the excited configuration from $nd\sigma_{lone-pair}$ to $nd\pi$, $nd\delta$, or $nd\sigma_{antibonding}$ becomes more stable. In fact, the ground state is predicted to be

$^4\Phi$: core$(nd\sigma_{bonding})^2(nd\sigma_{lone-pair})^1(nd\pi)^1(nd\delta)^1$
for TiH (group 4)

$^5\Delta$: core$(nd\sigma_{bonding})^2(nd\sigma_{lone-pair})^1(nd\pi)^2(nd\delta)^1$
for VH and NbH (group 5)

$^7\Sigma^+$: core$(nd\sigma_{bonding})^2(nd\sigma_{lone-pair})^1(nd\pi)^2(nd\delta)^2(nd\sigma_{antibonding})^1$
for MnH (group 7)

This does not happen in group 3 and 6 hydrides. Thus, it can be easily understood why the ground states in these hydrides have these leading configurations. However, no general rule has emerged for spin multiplicity, orbital angular momentum, or z component of the total angular momentum (Ω). These properties will be analyzed further after the inclusion of the results on group 8−12 hydrides in forthcoming papers.

4. Summary

The present paper reports the adiabatic and relativistic dissociation energy curves for low-lying spin-mixed states in monohydrides of groups 6 and 7 obtained by using the MCSCF+FOCI/SBKJC(f,p) method within the Z_{eff} approximation. The ground states of group 6 hydrides (CrH, MoH, and WH) have $\Omega = {}^1/_2(X^6\Sigma^+_{1/2})$, where Ω is the z component of the total angular momentum quantum number. Although the ground states of group 7 hydrides have $\Omega = 0^+$, their main adiabatic components are different; the ground state in MnH originates from $^7\Sigma^+$, while the main component is $^5\Sigma^+$ in TcH and ReH. Comprehensive sets of spectroscopic parameters, such as the dissociation energies, equilibrium distances, electronic transition energies, harmonic frequencies, anharmonicities, and rotational constants, are reported for several low-lying spin-mixed states in these hydrides. Large peak positions of electronic transitions were also estimated in each hydride. The periodic trends of the physical properties for group 3−7 hydrides have been discussed. Further investigations are continuing on the remaining group 8−12 hydrides. These will be reported shortly.[72]

Acknowledgment. Financial support from a grant-in-aid for Scientific Research (Nos. 11166231, 12042237, and 14077215) from the Ministry in Education, Science, Sports, and Culture, Japan (to S.K.), and from the U.S. Department of Energy (to M.S.G.). We are indebted to Dr. Dmitri G. Fedorov for his useful comments.

References and Notes

(1) Marenich, A. V.; Boggs, J. E. *J. Phys. Chem. A* **2004**, *108*, 10594.

(2) For example: *J. Comput. Chem.* **2002**, *23*, 8th issue.

(3) For example: Ermler, W. C.; Ross, R. B.; Christiansen, P. A. *Adv. Quantum Chem.* **1988**, *19*, 139.

(4) (a) Hay, P. J.; Wadt, W. R. *J. Chem. Phys.* **1985**, *82*, 270−283. (b) Wadt, W. R.; Hay, P. J. *J. Chem. Phys.* **1985**, *82*, 284−298. (c) Hay, P. J.; Wadt, W. R. *J. Chem. Phys.* **1985**, *82*, 299−310.

(5) (a) Stevens, W. J.; Krauss, M. *Chem. Phys. Lett.* **1982**, *86*, 320. (b) Stevens, W. J.; Basch, H.; Krauss, M. *J. Chem. Phys.* **1984**, *81*, 6026.

(c) Stevens, W. J.; Basch, H.; Krauss, M.; Jasien, P. *Can. J. Chem.* **1992**, *70*, 612. (d) Cundari, T. R.; Stevens, W. J. *J. Chem. Phys.* **1993**, *98*, 5555.

(6) Yarkony, D. R. *Int. Rev. Phys. Chem.* **1992**, *11*, 195.

(7) (a) Hess, B. A.; Marian, C. M.; Peyerimhoff, S. D. In *Modern Electronic Structure Theory*; Yarkony, D. R., Ed.; World Scientific: Singapore, 1995; Part I, p 152. (b) Marian C. M. *Problem Solving in Computational Molecular Science*; Wilson, S., Deircksen G. H. F., Eds.; Kluwer Academic: Dordrecht, 1997; p 291. (c) Marian, C. M. *Reviews in Computational Chemistry*; Lipowitz, K. B., Boyd, D. B., Eds.; Wiley-VCH: New York, 2001; Vol. 17, p 99.

(8) Matsushita, T.; Asada, T.; Koseki, S. Submitted for publication.

(9) Fedorov, D. G.; Koseki, S.; Schmidt, M. W.; Gordon, M. S. *Int. Rev. Phys. Chem.* **2003**, *22*, 551.

(10) Fedorov, D. G.; Schmidt, M. W.; Koseki, S.; Gordon, M. S. *Recent Advances in Relativistic Molecular Theory*; Hirao, K., Ishikawa, Y., Eds.; World Scientific: Singapore, 2004; Vol. 5, pp 107.

(11) Matsunaga, N.; Koseki, S. *Reviews in Computational Chemistry*; Lipkowitz, K. B., Larter, R., Cundari, T. R., Eds.; Indiana University-Purdue University at Indianapolis (IUPUI): Indianapolis, IN, 2004; Vol. 20, Chapter 2, pp 101.

(12) Koseki, S.; Schmidt, M. W.; Gordon, M. S. *J. Phys. Chem.* **1992**, *96*, 10768.

(13) Koseki, S.; Gordon, M. S.; Schmidt, M. W.; Matsunaga. N. *J. Phys. Chem.* **1995**, *99*, 12764.

(14) Matsunaga, N.; Koseki, S.; Gordon. M. S. *J. Chem. Phys.* **1996**, *104*, 7988.

(15) Koseki, S. Unpublished results for the sixth-row typical elements: Z_{eff}(Cs) = 12210, Z_{eff}(Ba) = 12432, Z_{eff}(Tl) = 9153, Z_{eff}(Pb) = 18204, Z_{eff}(Bi) = 18426, Z_{eff}(Po) = 18648, Z_{eff}(At) = 18870.

(16) Koseki, S.; Schmidt, M. W.; Gordon, M. S. *J. Phys. Chem.* **1998**, *102*, 10430.

(17) Koseki, S.; Fedorov, D. G.; Schmidt, M. W.; Gordon, M. S. *J. Phys. Chem. A* **2001**, *105*, 8262.

(18) Fedorov, D. G.; Gordon, M. S. *J. Chem. Phys.* **2000**, *112*, 5611.

(19) Schmidt, M. W.; Baldridge, K. K.; Boatz, J. A.; Elbert, S. T.; Gordon, M. S.; Jensen, J. H.; Koseki, S.; Matsunaga, N.; Nguyen, K. A.; Su, S.; Windus, T. L.; Dupuis, M.; Montgomery, J. A., Jr. *J. Comput. Chem.* **1993**, *14*, 1347.

(20) Fletcher, G. D.; Schmidt, M. W.; Gordon, M. S. *Adv. Chem. Phys.***1999**, *110*, 267.

(21) Gordon, M. S.; Schmidt, M. W. In *Theory and Applications of Computational Chemistry*; Dykstra, C., Ed., Elsevier; in press.

(22) Koseki, S.; Ishihara, Y.; Umeda, H.; Fedorov, D. G.; Gordon, M. S. *J. Phys. Chem. A* **2002**, *106*, 785−794 (Paper I).

(23) Koseki, S.; Ishihara, Y.; Umeda, H.; Fedorov, D. G.; Schmidt, M. W.; Gordon, M. S. *J. Phys. Chem. A* **2004**, *108*, 4707−4719 (Paper II).

(24) Bullock, R. M.; Song, J.-S. *J. Am. Chem. Soc.* **1994**, *116*, 8602.

(25) Luan, L.; Song, J.-S.; Bullock, R. M. *J. Org. Chem.* **1995**, *60*, 7170.

(26) Van Zee, R. J.; DeVore, T. C.; Weltner, W., Jr. *J. Chem. Phys.* **1979**, *71*, 2051.

(27) Xiao, Z. L.; Hauge, R. H.; Margrave, J. L. *J. Phys. Chem.* **1992**, *96*, 636.

(28) King, R. B. *Coord. Chem. Rev.* **2000**, *200*−*202*, 813 and references therein.

(29) Wang, X. F.; Andrews, L. *J. Phys. Chem. A* **2003**, *107*, 4081.

(30) Siegbahn, P. E. M. *Theor. Chim. Acta* **1993**, *86*, 219.

(31) Balasubramanian, K. *J. Chem. Phys.* **1990**, *93*, 8061.

(32) Wang, J. Z.; Balasubramanian, K. *J. Mol. Spectrosc.* **1989**, *138*, 204.

(33) Langhoff, S. R.; Pettersson, L. G. M.; Bauschlicher, C. W., Jr.; Partridge, H. *J. Chem. Phys.* **1987**, *86*, 268.

(34) Ruedenberg, K.; Schmidt, M. W.; Dombek, M. M.; Elbert, S. T. *Chem. Phys.* **1982**, *71*, 41, 51, 65.

(35) Schmidt, M. W.; Gordon, M. S. *Annu. Rev. Phys. Chem.* **1998**, *49*, 233.

(36) Lengfield, B. A., III; Jafri, J. A.; Phillips, D. H.; Bauschlicher, C. W., Jr. *J. Chem. Phys.* **1981**, *74*, 6849.

(37) Ehlers, A. W.; Boehme, M.; Dapprich, S.; Gobbi, A.; Hoellwarth, A.; Jonas, V.; Koehler, K. F.; Stegmann, R.; Veldkamp, A.; Frenking, G. *Chem. Phys. Lett.* **1993**, *208*, 111. (a) Exponents of 1.941, 1.043, and 0.823 are used for *f* functions on Cr, Mo, and W, respectively. (b) Exponents of 2.195, 1.134, and 0.869 are used for *f* functions on Mn, Tc, and Re, respectively.

(38) The *p* exponent is 1.0 for hydrogen.

(39) The effective nuclear charges of Cr, Mo, and W atoms are set to 11.64, 206.64, and 1074.48, respectively. Those of Mn, Tc, and Re atoms are 12.75, 214.14, and 1099.95, respectively. See refs 16 and 17.

(40) The total numbers of configuration state functions are 4 606 602 (CrH and MoH), 859 950 (WH), and 1 808 100 (MnH, TcH, and ReH). The estimated errors caused by the energy tolerance are about 2 (CrH), 19 (MoH), and 348 (WH) cm^{-1}, respectively, on the basis of second-order perturbation theory, using the largest matrix elements. The errors are 5 (MnH), 27 (TcH), and 401 (ReH) for group 7 hydrides.

(41) Colbert, D. T.; Miller, W. H. *J. Chem. Phys.* **1992**, *96*, 8061.

(42) The FOCI calculations in the ECP approaches for group 6 hydrides include 4 606 602 (CrH and MoH) and 859 950 (WH) configuration state functions and their spin−orbit matrixes includes 343 (CrH), 362 (MoH), and 277 (WH) adiabatic states. These numbers for group 7 hydrides are 1 808 100 (configuration state functions), 358 (MnH), 278 (TcH), and 326 (ReH).

(43) Chen, Clemmer, and Armentrout, *J. Chem. Phys.* **1993**, *98*, 4929.

(44) Wittborn, C.; Wahlgren, U. *Chem. Phys.* **1995**, *201*, 357.

(45) Cheng, W.; Balasubramanian, K. *J. Mol. Spectrosc.* **1991**, *149*, 99.

(46) Moore, C. E. *Atomic Energy Levels*; National Standand Data Ser., Nat. Bur. Stand.:Washington, DC, 1949, 1952, 1958; 35/Vols. I−III.

(47) Bauschlicher, C. W., Jr.; Ram, R. S.; Bernath, P. F.; Parsons, C. G.; Galehouse, D. *J. Chem. Phys.* **2001**, *115*, 1312.

(48) Bonatsos, D.; Daskaloyannis, C.; Drenska, S. B.; Karoussos, N.; Maruani, J.; Minkov, N.; Raychev, P. P.; Roussev, R. P. *Phys. Rev. A* **1999**, *60*, 253.

(49) Bonatsos, D.; et al. *Phys. Rev. A*: *At. Mol. Opt. Phys.* **1996**, *54*, 2533.

(50) Ram, R. S.; Bernath, P. F. *J. Mol. Spectrosc.* **1995**, *172*, 91.

(51) Ram, R. S.; Jarman; Bernath, P. F. *J. Mol. Spectrosc.* **1993**, *161*, 445.

(52) Dai, D.; Balasubramanian, K. *J. Mol. Spectrosc.* **1993**, *161*, 455.

(53) Brown; Beaton; Evenson *Astrophys. J. Lett.* **1993**, *414*, 125.

(54) Xiao, Z. L.; Hauge, R. H.; Margrave, J. L. *J. Phys. Chem.* **1992**, *96*, 636.

(55) Lipus; Bachem; Urban, *Mol. Phys.* **1991**, *73*, 1041.

(56) Corkery, S. M.; et al. *J. Mol. Spectrosc.* **1991**, *149*, 257.

(57) Shin, S.; Brugh, D. J.; Morse, M. D. *Astrophys. J.* **2005**, *619*, 407.

(58) Barone, V.; Adamo, C. *Int. J. Quantum Chem.* **1997**, *61*, 443.

(59) The "dsp" space includes the 4d and 5sp orbitals of molybdenum atom and 1s orbital of hydrogen. Unfortunately, the degeneracy is broken in the lowest ^{5}D state in the molybdenum atom in the dissociation limit, because the 5pπ orbitals of the molybdenum atom are replaced by external dπ orbitals during MCSCF orbital optimization.

(60) Xiao, Z. L.; Hauge, R. H.; Margrave, J. L. *J. Phys. Chem.* **1992**, *96*, 636.

(61) Balasubramanian, K.; Li, J. *J. Phys. Chem.* **1990**, *94*, 4415.

(62) Wang, X.; Andrews, L. *J. Phys. Chem.* A **2005**, *109*, 9021.

(63) $^5D_0$ correlates with the lowest Ω = (1/2) state of WH; $^5D_1$ with two Ω = (1/2) and the lowest Ω = (3/2) states; $^5D_2$ with two Ω = (1/2), two Ω = (3/2), and the lowest Ω = (5/2) states; $^7S_3$ with two Ω = (1/2), two Ω = (3/2), two Ω = (5/2), and the lowest Ω = (7/2) states; $^5D_3$ with two Ω = (1/2), two Ω = (3/2), two Ω = (5/2), and the lowest Ω = (7/2) states; and $^5D_4$ with two Ω = (1/2), two Ω = (3/2), two Ω = (5/2), two Ω = (7/2), and the lowest Ω = (9/2) states.

(64) The SOCI calculation of the W atom provides the energy difference of 3217 cm^{-1} between $^5D_0$ and $^7S_3$.

(65) Casarrubios, M.; Seijo, L. *J. Chem. Phys.* **1999**, *110*, 784.

(66) Garvey, J. F.; Kuppermann, A. *J. Phys. Chem.* **1988**, *92*, 4583.

(67) Wang, X.; Andrews, L. *J. Phys. Chem.* **2002**, *106*, 6720.

(68) Varberg, T. D.; Field, R. W.; Merer, A. J. *J. Chem. Phys.* **1990**, *92*, 7123.

(69) Gordona, I. E.; Appadoob, D. R. T.; Shayestehb, A.; Walkerb, K. A.; Bernath, P. F. *J. Mol. Spectrosc.* **2005**, *229*, 145.

(70) Balfour, W. J.; Launila, O.; Klynning, L. *Mol. Phys.* **1990**, *69*, 443.

(71) Balfour, W. J.; Lindgren, B.; Launila, O.; Oconnor, S.; Cursack, E. J. *J. Mol. Spectrosc.* **1992**, *154*, 177.

(72) Koseki, S.; Matsushita, T.; Gordon, M. S. In preparation.